Measurements of ^{10}Be and ^{26}Al production cross sections with 12 GeV protons by accelerator mass spectrometry

Seiichi Shibata and Mineo Imamura
Institute for Nuclear Study, University of Tokyo, Tanashi, Tokyo 188, Japan

Hisao Nagai
College of Humanities and Sciences, Nihon University, Setagaya-ku, Tokyo 156, Japan

Koichi Kobayashi
Research Center for Nuclear Science and Technology, University of Tokyo, Bunkyo-ku, Tokyo 113, Japan

Koh Sakamoto
Department of Chemistry, Kanazawa University, Kanazawa, Ishikawa 920-11, Japan

Michiaki Furukawa
Department of Chemistry, Nagoya University, Nagoya, Aichi 464-01, Japan

Ichiro Fujiwara
School of Economics, Otemon Gakuin University, Ibaragi, Osaka 567, Japan
(Received 22 June 1993)

The formation cross sections of ^{10}Be and ^{26}Al from Al, Fe, Co, Ni, Cu, Zn, Ag, and Au targets irradiated with 12 GeV protons were measured by accelerator mass spectrometry. The obtained cross sections were consistent with the excitation functions predicted from the literature values measured at other proton energies within the experimental uncertainties. The ^{10}Be cross sections increased with an increase in the target mass. On the other hand, the ^{26}Al cross sections decreased from Al to Ag targets, but increased somewhat from Ag to Au. The formation mechanisms of ^{10}Be and ^{26}Al including ^{7}Be, ^{22}Na, and ^{24}Na are discussed with respect to fitting of the experimental results to the calculated values using the universal formula of Campi *et al.* During the course of the discussion, we introduce a new parameter, the degree of neuton excess $(N-Z)/A$, in order to classify light fragments more clearly. It is found that the production of ^{10}Be and ^{24}Na with positive values for the degree of neutron excess can be well reproduced by the formula, indicating that fragmentation is a dominant process for ^{10}Be production from Fe to Au targets and for ^{24}Na from Ag to Au. However, the values calculated by the formula overestimate the yields of ^{7}Be, ^{22}Na, and ^{26}Al with negative values or zero for the neutron-excess parameter. Through a comparison of the calculated and experimental data it is also found that the cross section ratios of ^{10}Be/^{7}Be, ^{24}Na/^{26}Al, and ^{24}Na/^{22}Na are linearly correlated with the degree of neutron excess of the targets. This suggests that the production of ^{7}Be, ^{22}Na, and ^{26}Al with negative or zero $(N-Z)/A$ by a fragmentation process from Ag to Au targets is suppressed relative to those of ^{10}Be and ^{24}Na with positive values of the neutron-excess parameter.

PACS number(s): 25.40.Ep, 27.20.+n, 27.30.+t

I. INTRODUCTION

Long-lived nuclides ^{10}Be ($T_{1/2}=1.5\times10^{6}$ yr) and ^{26}Al (7.2×10^{5} yr) observed in terrestrial and extraterrestrial matters provide important keys to the deciphering of fossil records stored in those materials and allow investigations of their irradiation history by solar and galactic cosmic radiation. The production cross sections for these long-lived nuclides by high-energy protons are indispensable as basic nuclear data to solve the above-mentioned problems and to study the formation mechanism by spallation and fragmentation in high-energy reactions. However, accurate information concerning their cross sections still seems to be insufficient, mainly due to a difficulty to carry out low-level radioactivity measurements and/or conventional mass spectrometry that has usually been employed up to now to measure long-lived nuclides. Thus, satisfactory theoretical treatments to help understand the reaction mechanism, especially fragmentation, do not exist.

Recently, for trace analyses of long-lived nuclides such as ^{10}Be, ^{14}C, ^{26}Al, ^{36}Cl, ^{41}Ca, and ^{129}I accelerators have been applied as high-energy and extremely sensitive mass spectrometers [accelerator mass spectrometry (AMS)] in addition to the primary use of the accelerators as energetic particle sources. The usefulness of this method for both dating and trace element analysis has been pointed out by Muller [1], Nelson *et al.* [2], and Bennett *et al.* [3], although the first application of an accelerator to this mode had already been carried out more than 50 years ago by Alvarez and Cornog [4] for measuring ^{3}He and ^{3}H. We have applied this method to measurements of

^{10}Be and ^{26}Al produced not only in natural samples by interactions with cosmic radiation [5], but also in artificially irradiated targets with protons, neutrons, and bremsstrahlung from accelerators [6].

In this paper we report on the results for the production cross sections of ^{10}Be and ^{26}Al from aluminum, iron, cobalt, nickel, copper, zinc, silver, and gold with 12 GeV protons measured by an AMS system with the aid of an internal beam-monitor method [7]. The results were compared with those from AMS by Dittrich *et al.* [8,9], who have reported on the production of ^{10}Be and ^{26}Al from cosmochemically relevant elements ($Z \leq 28$) at $E_p = 0.1-2.6$ GeV, and with other earlier data.

On the basis of these data, we discuss the production mechanisms of ^{10}Be and ^{26}Al by spallation and fragmentation in high-energy nuclear reactions. Since a Monte Carlo simulation based on an intranuclear-cascade and evaporation model can reproduce the mass yield distribution from spallation, but not from fragmentation, we have analyzed the results using the universal formula for a fragment distribution produced by ~ 5 GeV protons derived by Campi *et al.* [10,11]. However, because of insufficient experimental data, it is not clear whether the formula is valid especially for small fragments produced by the fragmentation process. Our results therefore seem to be a good test concerning the use of the universal formula for predicting unknown cross sections for the production of residual nuclides with sufficient accuracy.

II. EXPERIMENTAL PROCEDURE

A. Irradiation

The irradiation was performed in the external primary beam line of the 12 GeV proton synchrotron at the National Laboratory for High Energy Physics (KEK), Japan. The number of incident protons was measured by the monitor reaction of ^{27}Al$(p,3pn)^{24}$Na, and was estimated to be 1.57×10^{14} for 10 min of irradiation. In calibrating the beam intensity, a value of 8.1 ± 0.9 mb was used as the cross section for the monitor reaction at $E_p = 12$ GeV. Each target foil, ranging in thickness from 8 to 58 mg/cm^2, was guarded on both sides with identical foils in order to compensate for recoil losses and to prevent cross-contamination between the targets. Samples having lighter mass nuclei were placed at the upstream side of the stack. Details of the irradiation were described in Ref. [12], in which the resultant cross sections for spallation products determined by nondestructive γ-ray countings were also reported.

B. Preparation of ^{10}Be and ^{26}Al samples

The target samples were dissolved in acid after adding 200 μg of beryllium and 500 μg of aluminum carriers. The beryllium fraction was separated by a cation exchange with $1M$ HCl and the aluminum fraction with $3M$ HCl. Before cation exchange separation, the target elements were removed by anion exchange, except for the aluminum and silver targets. The dissolved aluminum sample was charged on a cation exchange column without any preseparations. From the silver sample, AgCl was precipitated and filtered off. The separated beryllium and aluminum fractions were purified by precipitation of the hydroxides with aqueous ammonia. The beryllium solution in dilute HCl finally obtained was dried and redissolved in several drops of water containing 4% ^{17}O. The solution was then dried and ignited to BeO in vacuum. The aluminum hydroxide was redissolved in HCl containing a few micrograms of enriched ^{10}B; this solution was then evaporated and ignited to Al_2O_3 in an electric furnace. The blank samples were prepared from unirradiated target foils by the same chemical procedures as those for irradiated samples.

The BeO (or Al_2O_3) was mixed well with silver powder and compressed into a 1.5-mm-diam hole in a copper target cone of a cesium sputter source.

C. Accelerator mass spectrometry

The isotopic ratios of ^{10}Be/^{9}Be and ^{26}Al/^{27}Al were determined for the samples prepared as mentioned above by the AMS system using an internal beam-monitor method at the 4MV tandem Van de Graaff accelerator of the Research Center for Nuclear Science and Technology, University of Tokyo [13]. In the ^{10}Be/^{9}Be measurement, ^{9}Be^{17}O$^-$ served as a monitor beam for ^{10}Be^{16}O$^-$. The fraction of ^{9}Be^{17}O$^-$ was increased by labeling the BeO samples with enriched ^{17}O. In the case of ^{26}Al/^{27}Al, ^{26}Al$^-$ was monitored by measuring ^{10}B^{16}O$^-$ from the sputtering ion source.

The ratios of ^{10}Be/^{9}Be and ^{26}Al/^{27}Al were obtained by the following equations:

$$[^{10}\mathrm{Be}]_S/[^{9}\mathrm{Be}]_S = (1/\varepsilon_1)([^{10}\mathrm{Be}^{3+}]_D/[^{9}\mathrm{Be}^{3+}]_M) \times([^{9}\mathrm{Be}^{17}\mathrm{O}^-]_S/[^{9}\mathrm{Be}^{16}\mathrm{O}^-]_S) \quad (1)$$

and

$$[^{26}\mathrm{Al}]_S/[^{27}\mathrm{Al}]_S = (\varepsilon_2'/\varepsilon_2)(1/\varepsilon_3)([^{26}\mathrm{Al}^{3+}]_D/[^{16}\mathrm{O}^{2+}]_M) \times([^{10}\mathrm{B}^{16}\mathrm{O}^-]_S/[^{27}\mathrm{Al}^-]_S)\,, \quad (2)$$

where ε_1 and ε_3 are the transmission efficiencies from the high-energy analyzing magnet to the detector for ^{10}Be^{3+} and ^{26}Al^{3+}, and ε_2 and ε_2' those through the accelerator from ^{26}Al^{3+} and ^{16}O^{2+}, respectively; subscripts S, M, and D indicate the ion source, monitor, and detector. The transmission efficiencies (ε_1 and ε_3) were determined using standard samples of ^{10}Be (^{10}Be/^{9}Be$=4.98\times10^{-10}$) and ^{26}Al (^{26}Al/^{27}Al$=9.12\times10^{-10}$); values of 0.7–0.8 were obtained. The detector system comprised a silicon surface-barrier detector and an absorber containing nitrogen gas. The details of the AMS system and the measurement procedures were reported in Ref. [13].

III. RESULTS AND DISCUSSION

Figures 1 and 2 show the energy spectra of ^{10}Be and ^{26}Al measured for the nickel target, standard samples of ^{10}Be and ^{26}Al and chemistry-blank samples. In the ^{26}Al spectra, two other peaks due to ^{16}O^{2+} and ^{16}O^{4+} were assigned. The background levels in the ^{10}Be and ^{26}Al measurements were estimated to be about 5×10^{-14} and

1×10^{-13}, respectively, from the chemistry-blank sample spectra. The AMS measurements were repeated more than five times for each sample, and the reproducibilities for ^{10}Be and ^{26}Al measurements were found to be $\pm2.3\%$ and $\pm3.7\%$, respectively, using standard samples. A typical measurement time was 1000 s. The results of the AMS measurements are summarized in Table I.

The errors quoted in the cross sections include uncertainties in the amounts of beryllium and aluminum carriers added (1%), in the AMS measurements which mainly depend on counting statistics, and in the absolute isotopic ratios for ^{10}Be ($\pm1.5\%$) and ^{26}Al ($\pm2\%$) standard samples. Finally, the errors were estimated from these uncertainties and the ambiguity of reproducibility in the standard sample measurement by adding quadratically. Systematic uncertainties due to the beam-intensity calibration, estimated to be approximately 10%, were not included.

The cross sections obtained for 12 GeV protons in the present work are compared with earlier results at other proton energies from AMS and other methods in the following. The excitation functions for ^{10}Be and ^{26}Al produced from aluminum, iron, and nickel are shown in Figs. 3–5. For the production of ^{10}Be from aluminum [Fig. 3(a)], our result of 2.47 ± 0.16 mb is seen to be equal to those of 2.67 ± 0.17 mb at 1.2 GeV and 2.68 ± 0.17 mb at 2.6 GeV [8,9] within the experimental error. The production of ^{26}Al from aluminum is shown in Fig. 3(b). Earlier results by Furukawa *et al.* [14] using positron annihilation radiation with a low-level γ-γ coincidence spectrometer for E_p up to 52 MeV and AMS results by Schneider *et al.* (40–160 MeV) [15] and Dittrich *et al.* (0.1–2.6 GeV) [8,9] are also shown. Our result of 20.1 ± 1.6 mb at 12 GeV can be smoothly connected with those cross sections at lower E_p's, and agrees well with 20.0 ± 1.4 mb at 2.6 GeV. The ^{26}Al production from aluminum decreases with an increase in the incident proton energy up to several hundred MeV after the maximum value at about 25 MeV, and becomes almost constant in the GeV region.

For the production of ^{10}Be and ^{26}Al from iron, the results are shown in Figs. 4(a) and 4(b), respectively, along with the AMS results by Dittrich *et al.* [8,9]. In the case of ^{10}Be, the earlier measurements at 730 MeV (1.2 mb) from β-ray counting [16] and at 21 GeV (4.6 ± 0.8 mb) with conventional mass spectrometry [17] are also included; for the ^{26}Al production, the earlier result at 730 MeV (0.47 mb) [18] is shown. Both excitation functions for ^{10}Be and ^{26}Al increase up to a few GeV and subsequently level off in the higher GeV region. In the case of ^{10}Be production from nickel [Fig. 5(a)], our 12 GeV result is somewhat higher than the values at 2.6 GeV (2.58 ± 0.12

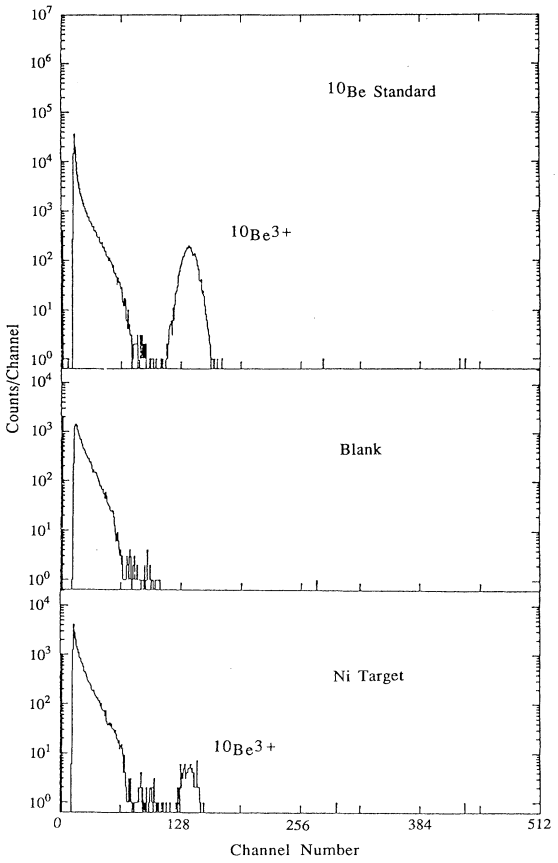

FIG. 1. Energy spectra of ^{10}Be for the samples of standard (^{10}Be/^{9}Be$=4.98\times10^{-10}$), chemistry-blank, and nickel target.

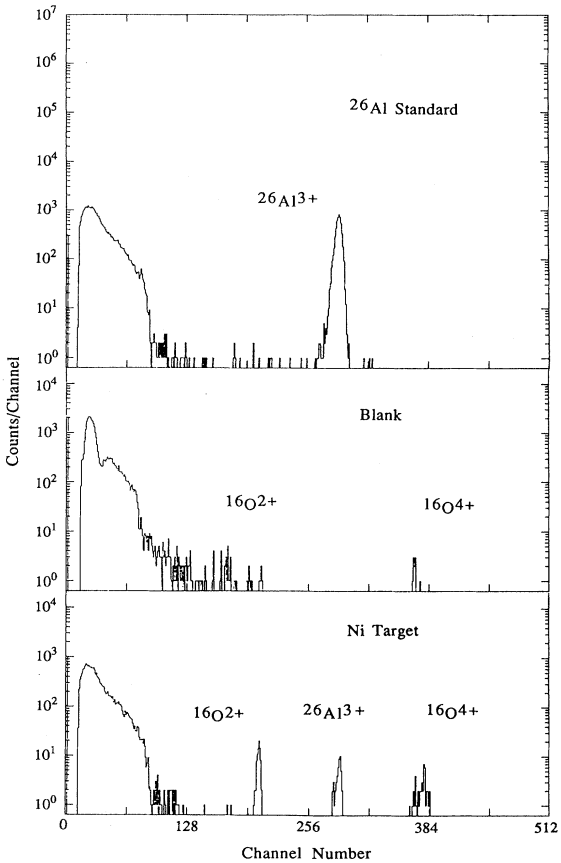

FIG. 2. Energy spectra of ^{26}Al for the samples of standard (^{26}Al/^{27}Al$=9.12\times10^{-10}$), chemistry-blank, and nickel target.

TABLE I. Results of accelerator mass spectrometry and estimated cross sections of ^{10}Be and ^{26}Al.

Target	Al	Fe	Co	Ni	Cu	Zn	Ag	Au
Thickness (mg/cm^2)	5.20	7.52	8.36	17.4	9.06	58.1	12.1	39.3
Be carrier (μg)	212.0	211.4	214.6	221.1	212.0	232.4	227.9	218.7
^{10}Be/^{9}Be ($\times 10^{-12}$)	3.171±0.182	2.653±0.283	3.581±0.317	7.605±0.455	3.934±0.380	24.68±1.03	9.035±0.574	53.18±2.04
^{10}Be (atom) ($\times 10^{7}$)	4.496±0.258	3.752±0.401	5.139±0.455	11.25±0.67	5.578±0.539	38.35±1.60	13.77±0.87	77.80±2.98
σ(^{10}Be) (mb)	2.47±0.16	2.95±0.33	3.83±0.36	4.02±0.27	4.14±0.42	4.57±0.23	13.0±0.9	41.3±2.0
Al carrier (μg)		533.9	511.8	512.5		574.3	478.5	530.7
^{26}Al/^{27}Al ($\times 10^{-12}$)	3.154±0.213	2.157±0.215	2.112±0.290	5.227±0.461		12.03±0.63	0.988±0.189	1.778±0.213
^{26}Al (atom) ($\times 10^{7}$)	36.55±2.47	2.567±0.256	2.410±0.331	5.975±0.527		15.40±0.81	1.054±0.201	2.104±0.252
σ(^{26}Al) (mb)	20.1±1.6	2.02±0.22	1.80±0.25	2.14±0.21		1.84±0.12	0.994±0.195	1.12±0.14

mb) [9] and at 3 GeV (2.2±0.5 mb) [19], while for ^{26}Al from nickel in Fig. 5(b) our value is slightly lower than the 2.6 GeV result [9]. However, the production of ^{10}Be and ^{26}Al from nickel seems to saturate at energies higher than several GeV, as in the cases of ^{10}Be and ^{26}Al from iron and ^{10}Be from aluminum.

Although measurements of ^{10}Be and ^{26}Al produced in high-energy reactions from cobalt, copper, zinc, silver, and gold, that are not entirely cosmochemically relevant target elements, have never been reported, the cross sections from these targets, especially medium to heavy elements such as silver and gold, are important for obtaining

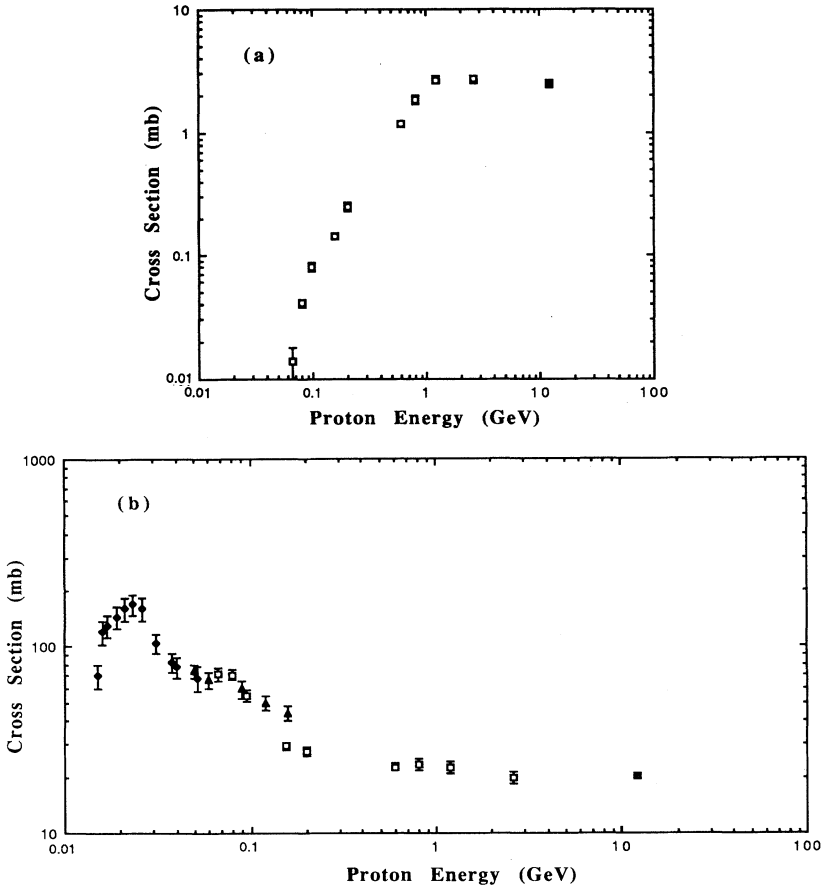

FIG. 3. (a) Excitation function for ^{27}Al(p,x)^{10}Be. The solid square denotes this work, and the open squares denote Refs. [8,9]. (b) Excitation function for ^{27}Al(p,pn)^{26}Al. The solid square denotes this work, the open squares Refs. [8,9], the solid diamonds Ref. [14], and the solid triangles Ref. [15].

information concerning the reaction mechanism. The productions from cobalt, copper, and zinc are expected to show almost the same trend as for iron and nickel. The excitation functions for ^{10}Be and ^{26}Al mentioned above, except for that for ^{26}Al from aluminum by the (p,pn) reaction with a low threshold, rise from the threshold energy and then level off at energies of several GeV. For silver and gold, the production cross sections of ^{10}Be and ^{26}Al also seem to gradually increase up to 12 GeV, analogous to the results for ^{7}Be, ^{22}Na, and ^{24}Na [12,20–23]. Measurements of ^{10}Be and ^{26}Al from these targets at lower proton energies should be carried out.

Figure 6 shows the cross sections (σ) of ^{10}Be and ^{26}Al produced by 12 GeV protons as a function of the target mass number (A). The ^{10}Be cross sections increase by more than one order of magnitude with an increase in the target mass from aluminum to gold, or the mass difference between the target and the product. On the other hand, those of ^{26}Al decrease by a factor of 20 from aluminum to silver, but increase somewhat from silver to gold. From similar plots for ^{7}Be and ^{22}Na production by

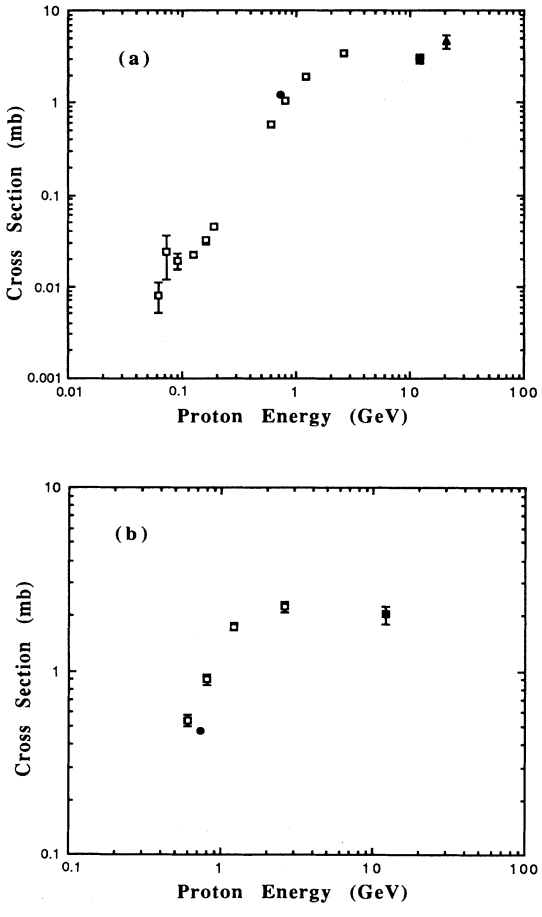

FIG. 4. (a) Excitation function for ^{nat}Fe$(p,x)^{10}$Be. The solid square denotes this work, the open squares Refs. [8,9], the solid circle Ref. [16], and the solid triangle Ref. [17]. (b) Excitation function for ^{nat}Fe$(p,x)^{26}$Al. The solid square denotes this work, the open squares Refs. [8,9], and the solid circle Ref. [18].

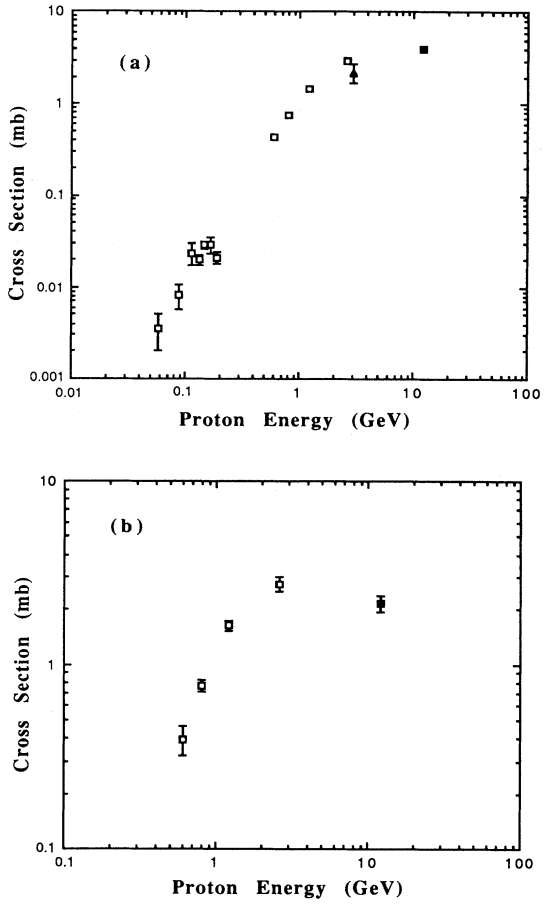

FIG. 5. (a) Excitation function for ^{nat}Ni$(p,x)^{10}$Be. The solid square denotes this work, the open squares Refs. [8,9], and the solid triangle Ref. [19]. (b) Excitation function for ^{nat}Ni$(p,x)^{26}$Al. The solid square denotes this work, and the open squares Refs. [8,9].

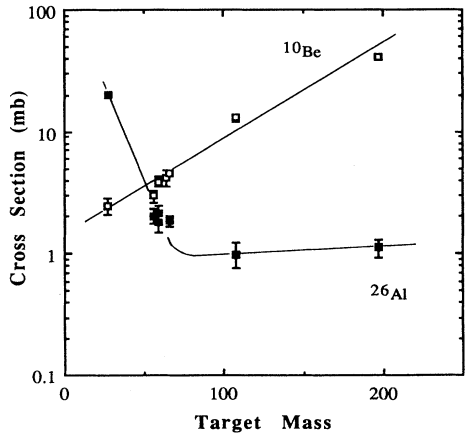

FIG. 6. Cross sections of ^{10}Be and ^{26}Al produced by 12 GeV protons as a function of target mass number. The solid line and curve are guides to the eye.

0.8–2.6 GeV protons [8], it has been speculated that the change in the slope of σ vs A reflects changing reaction mechanism for the production of ^{7}Be and ^{22}Na. Dittrich *et al.* [8] also noted that the change in the slope of the ^{22}Na cross sections at 2.6 GeV at $A \approx 55$ indicates a possible fragmentation process for the production of ^{22}Na from heavier targets. According to them, the change in the slope of the ^{26}Al production at a mass number of around 70 (Fig. 6) indicates the possible production of ^{26}Al by fragmentation in heavier targets, while being dominated by spallation in lighter ones. A large monotonic increase in ^{10}Be production from medium to heavier targets may also indicate that fragmentation is probably a dominant process. Consequently, it is qualitatively deduced that the dominant process for the production of ^{10}Be and ^{26}Al by high-energy protons changes from spallation to fragmentation with an increase in the slope from negative to positive in plots of the cross sections versus the target mass number. It is interesting to note that at a higher proton energy of 30 GeV [20] the production cross section of ^{7}Be from heavy elements (tantalum, gold, lead, and uranium) attains a constant value; that is, the positive slope changes to zero in the σ vs A correlation, probably due to a saturation effect for the production by fragmentation.

For a further discussion of the production mechanism, we compared our results with the calculated values from the following universal formula by Campi *et al.* [10]:

$$\sigma(x)=0.09X^{-2.5}+0.9\exp(3.7X) , \tag{3}$$

where X is the ratio of the fragment mass (K) to target mass (A) and $\sigma(x)$ is in units of mb. This formula implies that the mass yield for fragment K does not depend separately on the target and fragment mass, but only on the ratio $X=K/A$. They derived this formula by analyzing the fragment distribution produced by ~ 5 GeV protons on targets with $A \geq 60$ with two model-independent sum rules,

$$\sum_{K=1}^{A} \sigma(K)=\langle N \rangle \sigma_R \tag{4}$$

and

$$\sum_{K=1}^{A} K\sigma(K)=A\sigma_R , \tag{5}$$

where $\langle N \rangle$ is the total mean multiplicity of the fragments from a target of mass number A and σ_R is the total reaction cross section. For the total yield of fragments $K > 20$, they obtained the second term in formula (3) using an experimental mass-yield distribution, while the first term was introduced to estimate the remaining $K \leq 20$ contribution by assuming a power-law distribution ($K^{-\tau}$) for these light fragments [24]. Although it has also been pointed out by the authors [10] that the universal formula (3) is violated for a light target, such as ^{12}C, and that it is not clear whether the formula is valid for a very small fragment ($K \leq 10$), this formula includes contributions from both spallation and fragmentation for the fragment yield.

From the results given in Figs. 3–5 and the discussion above, the ^{10}Be and ^{26}Al production cross sections from aluminum to zinc are predicted to be almost constant in the energy region of 2–12 GeV. We therefore applied the formula to fit the target mass dependence of the ^{10}Be and ^{26}Al cross sections obtained at 12 GeV; the results are shown in Figs. 7(a) and 7(b), respectively. A similar

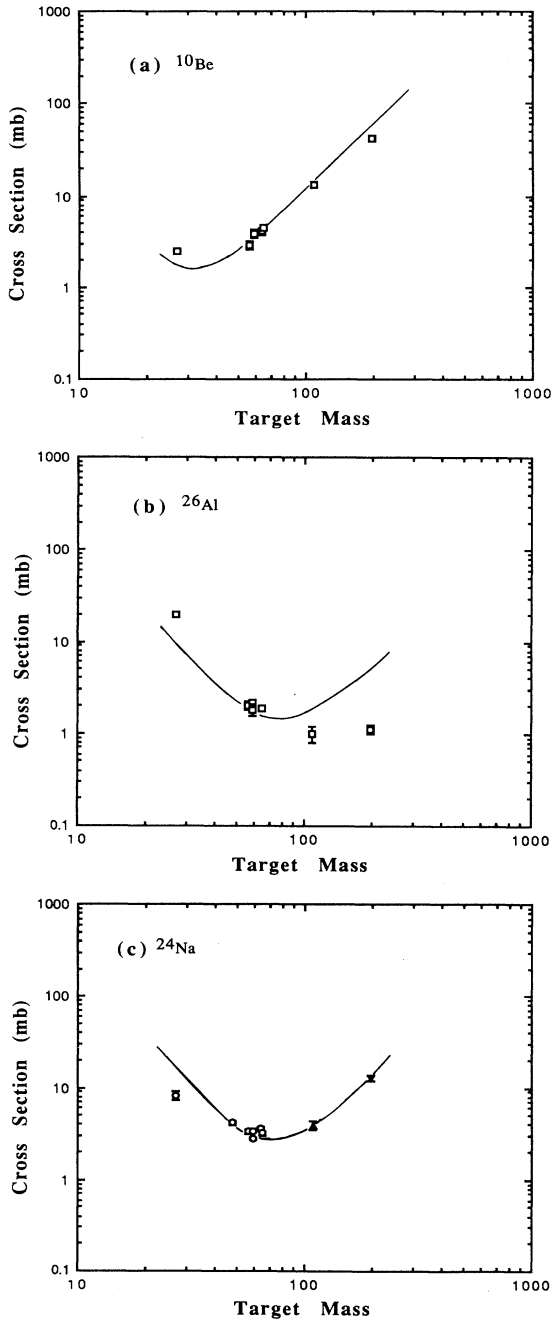

FIG. 7. Target mass dependencies of the cross sections for the formations of (a) ^{10}Be, (b) ^{26}Al, and (c) ^{24}Na at $E_p=12$ GeV. The open squares are experimental cross sections obtained in this work, the open circles Ref. [12], the solid triangle Ref. [22], and the solid inverted triangle Ref. [23]. The solid curves are predictions estimated by the universal formula [10]. For details see the text.

result for ^{24}Na in the same targets of aluminum to zinc [12] is shown in Fig. 7(c), including data from silver [22] and gold [23] targets at 11.5 GeV. ^{24}Na is one of the most accurately measured nuclides in the study of high-energy reactions. The measured cross sections of ^{10}Be, ^{26}Al, and ^{24}Na indicate the cumulative yields, while the calculated values from the formula are the total isobaric yields. We have assumed from the fitting of the calculated curve to the experimental data of iron to zinc that ^{10}Be collects 40% of the total mass yield for $K = 10$, ^{26}Al 34% for $K = 26$ and ^{24}Na 66% for $K = 24$; the solid curves shown in Figs. 7(a)–7(c) were obtained based on these assumptions. In the cases of ^{10}Be and ^{24}Na from iron to gold, excellent agreement with the results calculated by the formula was obtained, except for those from the aluminum target. The ^{24}Na yield from titanium [12] was also consistent with the calculated curve, as shown in Fig. 7(c). It is indicated that the lower limit of the target mass for applying the formula can possibly be extended to $A \approx 50$, lighter than the ~ 60 originally recommended in Ref. [10] and that the formula is valid for a fragment as small as $K = 10$. From the agreement for ^{10}Be and ^{24}Na, we can quantitatively estimate the ratio of the fragmentation yield to the total. In ^{10}Be, the ratios vary from 80 to 85% in iron to zinc, 96% in silver, to 99% in gold. Similarly, in ^{24}Na ratios from 15 to 25% in iron to zinc, 65% in silver to 93% in gold. This is evidence that fragmentation is a dominant process for ^{10}Be production from iron to gold and for ^{24}Na from silver to gold. However, in the case of ^{26}Al, the calculated curve overestimates by factors of 2–5 the experimental data from silver to gold, as shown in Fig. 7(b). Similar results to that of ^{26}Al were also obtained in the cases of ^{7}Be and ^{22}Na when comparing the calculated values obtained by the formula with the experimental data reported in Refs. [12,20,22,23]. Since the formula cannot reproduce the experimental results for ^{7}Be, ^{22}Na, and ^{26}Al, it is considered that the contribution of the fragmentation process is suppressed for the production of these three nuclides from silver to gold in this energy region.

Why are the yields of these nuclides by fragmentation lowered relative to those of ^{10}Be and ^{24}Na in medium to heavy elements? The overestimate by the formula is of interest in the correlation with the neutron to proton ratios (N/Z) of the product nuclides. The ratios of ^{7}Be $(N/Z = 0.75)$, ^{22}Na (1.0), and ^{26}Al (1.0) are smaller than those of ^{10}Be (1.5) and ^{24}Na (1.18). Here, we introduce the degree of neutron excess defined by $(N-Z)/A$, where $A = N+Z$, in order to classify these five nuclides more clearly than the neutron to proton ratio, since the expression of a neutron-rich or proton-rich nuclide is sometimes ambiguous, especially for light nuclides. The universal formula is valid for ^{10}Be $[(N-Z)/A = 0.2]$ and ^{24}Na (0.08) with positive values, but not for ^{7}Be (-0.14), ^{22}Na (0) and ^{26}Al (0) with negative or zero values. Furthermore, the degree of neutron excess of the products is shown to correlate with those of the target elements. The cross section ratios for ^{10}Be/^{7}Be and ^{24}Na/^{26}Al as a function of $(N-Z)/A$ of the target elements are given in Fig. 8. Both ratios increase by a factor of about 10 with an increase in the degree of neutron excess of targets from 0.05 to 0.2; the solid lines, drawn as guides to the eye, are almost parallel. The results for the ratios of ^{24}Na/^{22}Na estimated by the values in Refs. [12,20,22,23] are also indicated by the dashed line in Fig. 8. The ratios increase with an increase in the degree of neutron excess of the targets, as in the cases of ^{10}Be/^{7}Be and ^{24}Na/^{26}Al, although the slope of the dashed line is smaller than those of the solid lines. It is confirmed from the figure that fragmentation yields of ^{7}Be, ^{22}Na, and ^{26}Al with $(N-Z)/A \leq 0$ from target elements with large neutron excess are relatively lower compared with those of ^{10}Be and ^{24}Na with $(N-Z)/A > 0$. The cross section ratios of ^{24}Na/^{22}Na from silver [25] and gold [23] at $E_p = 300$ GeV agree well with those from the same targets at 30 GeV [20], which is shown by the dotted line including the ratio from copper at 30 GeV [20] in Fig. 8. The slope of the dotted line is almost parallel to the solid ones. When the production of these nuclides reaches saturation in high-energy reactions, it is suggested that the production ratios of these nuclides as a function of the degree of neutron excess of target lie on lines with the same slope. It should also be noted that the correlation lines between the cross section ratios of ^{10}Be/^{7}Be and $(N-Z)/A$ of

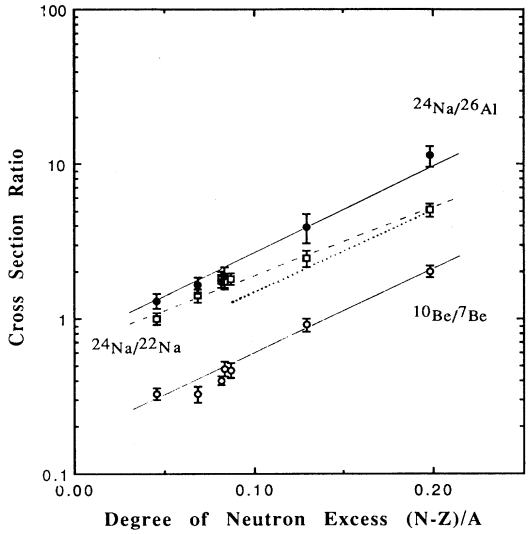

FIG. 8. Cross section ratios for ^{10}Be/^{7}Be (open circles), ^{24}Na/^{26}Al (solid circles), and ^{24}Na/^{22}Na (open squares) at $E_p = 12$ GeV as a function of the degree of neutron excess $(N-Z)/A$ of the target elements iron, cobalt, nickel, copper, zinc, silver, and gold. The cross sections for ^{10}Be and ^{26}Al were obtained in this work. The ^{7}Be, ^{22}Na, and ^{24}Na data from iron to zinc targets are taken from Ref. [12] and those from silver Ref. [22]. The ^{7}Be from gold is an average value of the data from tantalum, lead, and uranium targets in Ref. [20]. The ^{22}Na and ^{24}Na from gold are taken from Ref. [23]. The solid lines are guides to the eye for ^{10}Be/^{7}Be and ^{24}Na/^{26}Al, and the dashed line for ^{24}Na/^{22}Na. The dotted line is for ^{24}Na/^{22}Na from copper, silver, and gold targets at $E_p = 30$ GeV [20] and from silver [25] and gold [23] at $E_p = 300$ GeV. The ratios from silver and gold at 30 GeV agree well with those at 300 GeV, and the ratios from gold at 30 and 300 GeV are also consistent with that from gold at 12 GeV.

manganese, iron, and nickel targets at 0.8, 1.2, and 2.6 GeV [8] are almost parallel to the solid line at 12 GeV in Fig. 8; in the case of 2.6 GeV, the line is almost identical to the one obtained at 12 GeV in $0.046 < (N-Z)/A < 0.091$ of the targets. For a further elucidation of the implications of the correlations exemplified in Fig. 8, more experimental investigations, especially accurate measurements of these light fragments produced from medium to heavy elements, are required.

IV. CONCLUSION

We measured the production cross sections of the long-lived nuclides ^{10}Be and ^{26}Al by AMS using targets irradiated at $E_p = 12$ GeV. The obtained results were compared with data for ^{7}Be, ^{22}Na, and ^{24}Na appearing in the literature, and analyzed by the universal formula of Campi *et al.* [10]. The experimental results for ^{10}Be and ^{24}Na with positive values for the degree of neutron excess $[(N-Z)/A]$ could be well reproduced by the formula, but not ^{7}Be, ^{22}Na, and ^{26}Al with negative or zero for the degree of neutron excess. From the analysis, it is indicated that fragmentation is a dominant process for ^{10}Be production from iron to gold targets and for ^{24}Na from silver to gold. On the other hand, the yields of ^{7}Be, ^{22}Na, and ^{26}Al from silver to gold are lower than the calculated values by the formula, suggesting that the contribution of the fragmentation process is suppressed for the production of ^{7}Be, ^{22}Na, and ^{26}Al from medium to heavy elements. It is also found that the cross section ratios of ^{10}Be/^{7}Be, ^{24}Na/^{26}Al, and ^{24}Na/^{22}Na increase with an increase in the $(N-Z)/A$ of the targets. It may therefore be concluded that yields of light fragments with negative or zero for the degree of neutron excess by fragmentation of medium to heavy elements with large neutron excess are suppressed relative to those of light products with positive values of the degree of neutron excess. Also, based on the correlation shown in Fig. 8, one can roughly estimate the cross section of either one of the ratios from others measured in the GeV region, especially ^{10}Be cross section from ^{7}Be and those of ^{26}Al and ^{22}Na from ^{24}Na. Although more experimental investigations for light fragments produced by high-energy reactions are needed, the information obtained in this study can undoubtedly provide important clues for elucidating the reaction mechanism as well as constructing theoretical models for high-energy reactions.

ACKNOWLEDGMENTS

We wish to thank Dr. M. Numajiri, Professor K. Kondo, KEK, and Professor S. Mori, University of Tsukuba, for kindly supplying the irradiated samples for the present work. We would also like to express our thanks to H. Yamashita, University of Tokyo, for his helpful cooperation in the AMS measurements.

[1] R. A. Muller, Science **196**, 489 (1977).
[2] D. E. Nelson, R. G. Korteling, and W. R. Stott, Science **198**, 507 (1977).
[3] C. L. Bennett, R. P. Beukens, M. R. Glover, H. E. Gove, R. B. Liebert, A. E. Litherland, K. H. Purser, and W. E. Sondheim, Science **198**, 508 (1977).
[4] L. W. Alvarez and R. Cornog, Phys. Rev. **56**, 379 (1939).
[5] H. Nagai, T. Kobayashi, M. Honda, M. Imamura, K. Kobayashi, K. Yoshida, and H. Yamashita, Nucl. Instrum. Methods B **29**, 266 (1987).
[6] M. Imamura, H. Nagai, M. Takabatake, S. Shibata, K. Kobayashi, K. Yoshida, H. Ohashi, Y. Uwamino, and T. Nakamura, Nucl. Instrum. Methods B **52**, 595 (1990).
[7] M. Imamura, Y. Hashimoto, K. Yoshida, I. Yamane, H. Yamashita, T. Inoue, S. Tanaka, H. Nagai, M. Honda, K. Kobayashi, N. Takaoka, and Y. Ohba, Nucl. Instrum. Methods B **5**, 211 (1984).
[8] B. Dittrich, U. Herpers, M. Lüpke, R. Michel, H. J. Hofmann, and W. Wölfli, Radiochim. Acta **50**, 11 (1990).
[9] B. Dittrich, U. Herpers, H. J. Hofmann, W. Wölfli, R. Bodemann, M. Lüpke, R. Michel, P. Dragovitsch, and D. Filges, Nucl. Instrum. Methods B **52**, 588 (1990).
[10] X. Campi, J. Desbois, and E. Lipparini, Phys. Lett. **138B**, 353 (1984).
[11] J. Hüfner, Phys. Rep. **125**, 129 (1985).
[12] T. Asano, Y. Asano, Y. Iguchi, H. Kudo, S. Mori, M. Noguchi, Y. Takada, H. Hirabayashi, H. Ikeda, K. Katoh, K. Kondo, M. Takasaki, T. Tominaka, and A. Yamamoto, Phys. Rev. C **28**, 1718 (1983).
[13] K. Kobayashi, M. Imamura, H. Nagai, K. Yoshida, H. Ohashi, H. Yoshikawa, and H. Yamashita, Nucl. Instrum. Methods B **52**, 254 (1990).
[14] M. Furukawa, K. Shizuri, K. Komura, K. Sakamoto, and S. Tanaka, Nucl. Phys. **A174**, 539 (1971).
[15] R. J. Schneider, J. M. Sisterson, A. M. Koehler, and R. Middleton, Nucl. Instrum. Methods B **29**, 271 (1987).
[16] M. Honda and D. Lal, Nucl. Phys. **51**, 363 (1964).
[17] C. Perron, Phys. Rev. C **14**, 1108 (1976).
[18] M. Honda and D. Lal, Phys. Rev. **118**, 1618 (1960).
[19] G. M. Raisbeck, P. Boerstling, R. Klapisch, and T. D. Thomas, Phys. Rev. C **12**, 527 (1975).
[20] J. Hudis and S. Tanaka, Phys. Rev. **171**, 1297 (1968).
[21] R. Wölfle and S. M. Qaim, Radiochim. Acta **50**, 185 (1990).
[22] G. English, N. T. Porile, and E. P. Steinberg, Phys. Rev. C **10**, 2268 (1974).
[23] S. B. Kaufman, M. W. Weisfield, E. P. Steinberg, B. D. Wilkins, and D. Henderson, Phys. Rev. C **14**, 1121 (1976).
[24] J. E. Finn, S. Agarwal, A. Bujak, J. Chuang, L. J. Gutay, A. S. Hirsch, R. W. Minich, N. T. Porile, R. P. Scharenberg, B. C. Stringfellow, and F. Turkot, Phys. Rev. Lett. **49**, 1321 (1982).
[25] N. T. Porile, G. D. Cole, and C. R. Rudy, Phys. Rev. C **19**, 2288 (1979).